Scientific Research Publishing

Open Journal of Biophysics, 2021, 11, 133-146
https://www.scirp.org/journal/ojbiphy
ISSN Online: 2164-5396
ISSN Print: 2164-5388

The Spreading Depression Propagation: How Electrochemical Patterns Distort or Create Perception

Vera Maura Fernandes de Lima[1], Alfredo Pereira Junior[2], Guilherme Lima de Oliveira[3]

[1]Centro de Biotecnologia CNEN/IPEN-SP, São Paulo, Brazil
[2]Department of Human and Nutritional Sciences, Biosciences Inst., UNESP, Botucatu, São Paulo, Brazil
[3]São Paulo, São Paulo, Brazil
Email: vmflima@ipen.br, guivillares@gmail.com, alfredo.pereira@unesp.br

How to cite this paper: de Lima, V.M.F., Pereira Jr., A. and de Oliveira, G.L. (2021) The Spreading Depression Propagation: How Electrochemical Patterns Distort or Create Perception. *Open Journal of Biophysics*, **11**, 133-146.
https://doi.org/10.4236/ojbiphy.2021.112003

Received: November 26, 2020
Accepted: February 5, 2021
Published: February 8, 2021

Abstract

At the transition from quiescence to propagating waves recorded in isolated retinas, a circular electric current closes in the extracellular matrix; this circular current creates a magnetic torus flow that, when entering quiescent tissue in front of the wave, recruits elements and when leaving behind, helps to build the absolute refractory state. The waving magnetic torus is the consequence of the vortex effect and explains the energy boost that drives propagation. **Methods:** We interpret experimental results from intrinsic and extrinsic fluorescence dyes, voltage, calcium and pH sensitive, optical signals from isolated retinas, and time series recordings using ion exchange resins: Ca, K, pH, Na, Cl recorded extracellularly at retinas, cerebellums and cortices coupled to spreading depression waves. Finally, we checked the ECoG activity, also a time series, at the transition from after discharges to spreading depression in rat hippocampus. **Results:** The integrated assessment of the diversified measurements led to the realization that the magnetic flow at the wavefront is a major contributor to the wave propagation mechanisms. This flow couples mass and charge flows as a swirling torus from excited to quiescent tissue. **Conclusions:** An alternative model of the brain is possible, apart from the classical HH and molecular biology model. Physical chemistry of charged gels and its flows explains the results. The conceptual framework uses far from equilibrium thermodynamics.

Keywords

Brain Electrochemistry, Retinal Model, Resonance, Spreading Depression, Functional CNS Syndromes, Vortex Effect

1. Introduction

The power of the vortex effect in separating matter and energy is known to mankind since millennia. Our species learned how to use it since antiquity, in obtaining drinking water and air conditioning buildings in desertic regions [1]. In this manuscript, we will argue that spreading depression propagation can teach us how the brain works, in the sense of linking electrochemical dynamical patterns to perceptual correlates. Furthermore, we will argue that wave propagation can be explained by the vortex effect.

The spreading depression wave is an emergent property of central gray matter and its existence is demonstrated in all parts of it, from spinal chord to neocortex, for reviews, see [2] [3] [4] [5]. The phenomenon was discovered in 1940 by Aristides Leão, who grasped the implication of his discovery in the understanding of the physiopathology of functional syndromes of the CNS. Lashley, in the same year, predicted such a wave, calculated its propagation velocity and made the same inference about its importance that Leão did. The tittle of his paper says: "Patterns of cerebral integration indicated by the scotomas of migraine" [6]. Therefore, in 1940 it was clear that waves propagated in gray matter and that they had perceptual correlates in the form of distorted perception.

The scotomas of occipital migraines present themselves as bright bars that travel in the visual field followed by a dark spot that grows. The bright part is the front, with a dire price in energy expenditure. For example, there is dissipation of energy in the form of heat and infrared photons liberation [3] [5] [7]. The dark patch is the tissue in absolute refractory state. Like the retinal spreading depression, the action potential is also an excitation wave, has excited and refractory states and expends energy [7] [8] [9]. Both have macroscopic spatial scales and the difference in temporal scale is irrelevant in the context discussed here.

In this text we will argue that magnetic flow within the brain explains not only spreading depression waves propagation. They could be the key to understand perception.

2. Methods

In order to conclude the key role of the magnetic flow in spreading depression waves propagation, we examined decades of diversified data, such as image processing of intrinsic optical signals [Note 1] (IOS) and extrinsic fluorescence dyes Ca, voltage and pH sensitive. As well as time series displaying the ion activity in the extracellular space of the neuropil (inner plexiform layer) in isolated retinas and compared the same type of results from cerebellum and cortices. Finally, we realized that if the conjecture about the influence of the geometry of the glial network was correct, then, the vortex effect would be seen at the frontwave of spreading depressions in the rat hippocampus in the form of split frequencies typical of Von Karmann street effects [Note 2]. A previous study that examined the ECoG of rat hippocampi and recorded with sampling rates of 700 Hz was examined and the split frequencies (up to 250 Hz) observed during

the energy expenditure typical of spreading depressions wavefronts [10].

3. Experimental Results

3.1. Mass and Charge Flows Associated with Spreading Depression Waves

The experimental results discussed here (most of it) concern data from two models: the isolated chick retina and the *in situ* rat hippocampus. In the vertebrate retina, the Intrinsic Optical Signal (IOS) associated with retinal spreading depression waves (RSDs) is macroscopic [Note 1], making this preparation unique for the observation of its propagation. The most probable patterns are solitary circular waves and logarithm spirals. Circular spirals were rarely seen and stay mostly in place with a little jitter, whereas the logarithm spirals wander around the retina creating another level of abstract patterns (see [11]). Circular, two dimensional propagation can be taken mathematically as a special case of a dynamic spiral pattern propagation.

Figure 1 and **Figure 2** show the birth and propagation of a solitary circular retinal wave. At the inset the figure shows two time series that were recorded simultaneously with the video in the Picture In Picture (PIP) mode. One series records the extracellular potential at the electrode tip, the second the mean bright brightness of a square pixel matrix with 50 μm side length overlaying the electrode tip. This time series shows the optical changes or the Intrinsic Optical Signal (IOS). Note that the field potential leads the IOS in this wave (shown in **Figure 2**). This pattern is frequent; however, also frequent is the simultaneous rise of both signals.

Ten seconds later the wave is a large circle of optical changes, what one sees is the loss of retina transparency and consequent increase in light scatter. **Figure 2** shows how the extracellular drop of potential (by historical convention in electrophysiology, negativity is up and due to autoscaling of the recording system, one sees the time series moving in the downward direction) relates to the optical changes in tissue around the electrode tip. Remembering from the previous figure, the wave propagates at the rate of 45 μm/sec. It exactly at this distance from the electrode tip that the wave changes the extracellular potential. One second later that dV/dt will peak (frames 127 - 129). It is at this time that the dIOS/dt catches up and also peaks.

Figure 1 and **Figure 2** show a circle of increase in light scatter; however, the IOS associated with membrane excitation have light scatter and birefringence variations [9] [12] tightly coupled to ionic activity changes.

The temporal evolution of ionic activity associated with wave propagationresult in time series in most experiments. The following relationship exists among them: the peak of the dV/dt = d[k]/dt = d[Na]/dt whereas d[Ca]/dt begins at the peak of dV/dt (see for example [3] [4] [5] [12] [13]).

The calcium activity variation is tightly coupled to a component of the pH changes. This component happens at the frontwave and has a kinetics of seconds and thus cannot be associated with metabolism. It must be something else. Our

interpretation is that protons and hydronium ions "disappearance" is the result of dissociated water becoming liquid water. Therefore, the pH shift at the front wave, or at least the major part of it.

The dissociated water makes the Exclusion Zone (EZ) at membranes; this state of water is denser than the liquid and has birefringence [14]. Both calcium activity and pH changes were recorded in RSDs as changes in fluorescence images [2] [4] [5] [12]. The novelty here was that wave patches of tissue could lack the ionic change response maintaining the light scatter at 545 nm. A second slow pH change associated with RSDs is metabolic-production and secretion of lactic acid by microglia, the kinetics follow the second optical component of the optical profile of RSDs [2] [5] the time scale is minutes. In summary: the ionic activity changes in the frontwave are all compatible with the proposed charged gel (EZ) changes and that includes the early alkalinization that lacks explanation in the HH membrane model of same data.

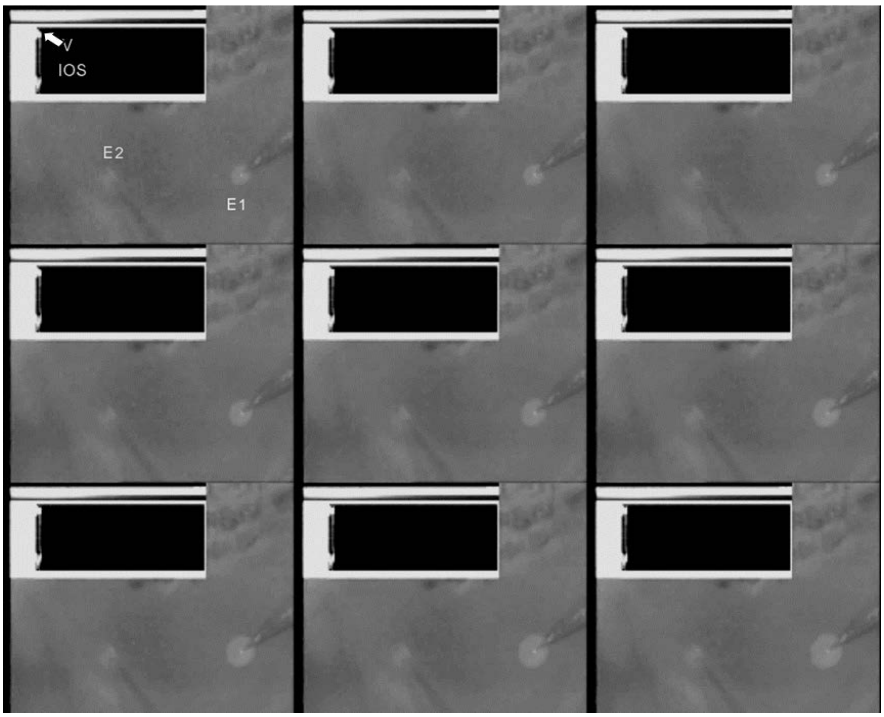

Figure 1. E1 is the stimulating electrode, a glass pipette filled with NaCL. It is positioned very close to the vitreal surface but does not touch it. Rectangular voltage pulses stimulate the tissue and create sharp pulse transients in the PIP time series display. E2 is the recording electrode. It is also a glass pipette filled with KCl solution the electrode tip is inserted in the inner plexiform layer within the extracellular matrix of the tissue. The typical pipettes tips were 20 - 50 μm diameter for both stimulating and recording electrodes. The montage of frames shows the first second of a record. In each row 100 msec in time separates the frames, between columns, 300 msec is the time interval. The inset picture in picture (PIP), shows the two time series recorded simultaneously: above is the extracellular potential labeled V (arrow) in the first frame and below the time series shows the microscale IOS. It shows the average brightness of square pixel matrix about 50 × 50 μm area. The area is above and the closest possible to the recording electrode tip. Note the electrical stimulus artifact in the extracellular potential recording.

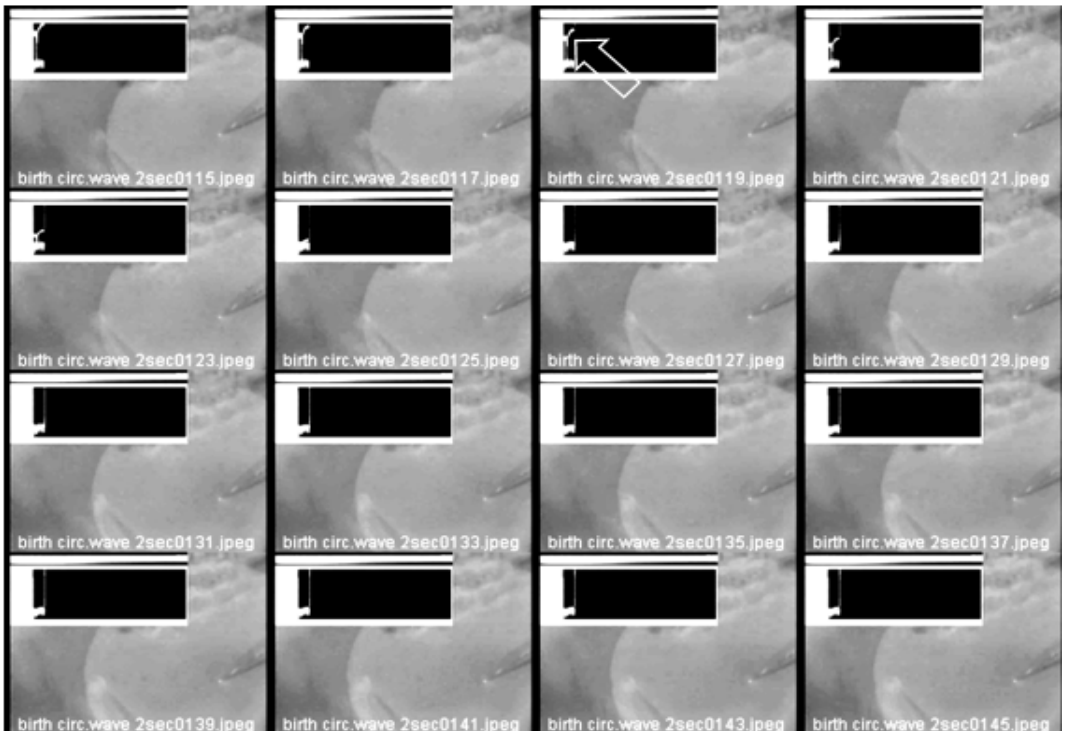

Figure 2. Same experiment showed in the previous figure, 10 seconds propagation later when the circular wave invades the recording electrode sampling space. The time between frames in the same row is 200 msec and 600 msec between columns. The montage shows the recorded time series, extracellular potential [V in previous figure] and the IOS as in the previous figure at their maximum rate of change. Valid for the extracellular potential and optical changes variables due to their tight coupling. **First row**, the near surface stimulating electrode [E1 of previous figure] is to right of the viewer. The inserted recording electrode [E2] on the left. The third frame of the first row, shows the frame when the recording electrode sensed the electromagnetic field of the propagating wave (arrow). Note that the extracellular field potential precedes any changes in the IOS time series. At frame numbered 119 the time series labelled V starts to move with no change in the time series labelled IOS. This displayed pattern is frequent. **Second row**, the wave is close to the tip of the recording electrode. At the second frame the two time series coincide in the display, frame 125. The extracellular voltage drop and the optical changes therefore coincide and grow together. **Third and Fourth rows**, the recording electrode tip is behind the propagating front. The two variables [V and IOS] keep growing together. Due to autoscaling of the display program, the single trace fills the display. The extracellular potential drop is upright because of convention in electrophysiological recordings. Waves recorded in similar experimental contexts, had the peak of potential drop and optical changes 6 - 8 seconds after the initial growth (see [22]). The figure shows the two variables reaching the maximum rate of change. In similar waves, the mean for this maximum is set at 1.8 - 2 seconds after the initial change [22]. The propagation velocity calculated for this wave was 2.7 mm/min, close to the 3 mm/min gran mean across thousands of experiments from several laboratories for temperatures 29 to 32 C.

The kinetics of potassium activity and potential drop are tightly coupled in spreading depression waves; to the point that many researchers attributed entirely to potassium channels activity the potential drop (see for example [13]). Not only that, the potential and ion activity changes have the same signal at both sides of the macroglial membranes. The same is true for the early pH shift, the same alkalinization happens at both sides of glial cells membranes.

The latter variables early pH and potassium activity variables are also tightly coupled to the optical properties changes in chick retinas. In chick retinas in particular a structural feature is of importance: about 2/3 of the length of the Müller cells are divided in fine tubes [5] these tubes have no organelles like mi-

tochondria but are filled with intermediate filaments made of GFAP (Glial Fibrillary Acidic Protein) see also [14]. The telltale part is the acidic mention. In here we assume that around the stack of the acid fibrils, water dissociates and creates and EZ (exclusion zone) [15]. Among the properties of EZs is birefringence. At the quiescence/excited state transition this EZ relaxes and in consequence, the Müller cells lose their lightguide role transiently due to birefringence loss [12] [16] [17] and light scatter increases creating the optical changes or IOS.

In other words, the frontwave releases energy. It does so in several forms of flows, in which water flows are an important part both liquid and dissociated water (for example hydronium ions), free cations and semi mobile anions (radicals in membrane carbohydrates and proteins). The macroscopic circular current that arises at the transition to propagating wave releases red/near infrared light besides heat [8] and when propagation begins green light scatter appears (505 - 540 nm) [5] [12]. We observed this transition many times with voltage sensitive dyes and looking at the Intrinsic Optical Signal (IOS) with infrared and black/white cameras associated with optical filters (see Fig. 9 to Fig. 11 of [5]). We discovered that the red/near infrared scatter followed the potential distribution, therefore a circular linear pattern implies a circular current. When waves were elicited by a light mechanical touch, standing patterns of IOS emerged around the stimulated area and preceded the circular current (see Fig. 17 and Fig. 19 of [2]).

The purpose of **Figure 3** and **Figure 4** is to show how the transition can be followed by observing the tissue IOS.

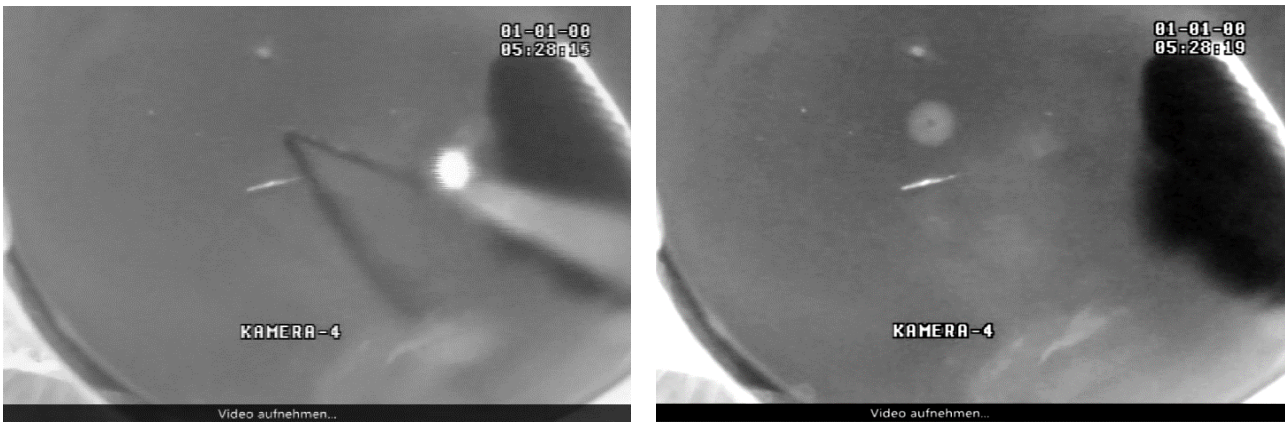

Figure 3. Mechanical stimulation left and circular wave right. Left frame, the frame shows the moment when a tungsten needle (50 μm tip) touches the retinal surface. The eyecup was cut at the equator and glued to a dish. A videocamera records from above. The large structure in the lower right is the pecten, its foot is continuous with the sclera. The length of the pecten foot shown in the frame is 1.8 mm. The pecten consists of blood vessels covered by pigmented epithelium and thus assumed to transport nutrients for this avascular retina. The stimulus is at central retina in a flat region of the chick retina. Right frame 3 seconds later a perfect circular wave is propagating around the stimulation point. Its diameter is 300 μm. Solitary circular waves like this one are the most probable outcome after stimulation. They will invade the whole of the retina without changing the uniform velocity of spread or the brightness of the IOS even after drastic structural changes in the tissue: in front of the pecten is the optical papilla, the exit of the optical nerve fibres. It is a semi-circular area extending from the tip of the pecten to 250 μm in front of it. At this point the tissue consists of only macroglia (Müller cells) and myelinated axons. This change does not affect propagation velocity of retinal waves or its brightness. Therefore, that macroglia dominates the IOS is a foregone conclusion.

Figure 3 (left frame) shows a mechanical stimulation of central retina using a tungsten needle (50 μm). Pressing a charged (piezoelectric) gel will move charges, therefore, mechanical and electrical stimulation are very similar. The mechanical one has an exact point of stimulation, showed in Figure 3. Close to three seconds later, a full blow, perfectly circular propagating wave is present around the stimulation point. The diameter of this wave is 300 μm. Figure 4(a) to Figure 4(f) follow the transition. In the stimulated region a standing dynamical pattern arises hundreds of milliseconds after the touch. The light scatter associated with it contains only red/near-infrared wavelengths. The dynamic character of the spatial pattern conveyed in shimmering bright points inside it and in lower frequency space/time oscillations of brightness of the whole pattern. When a circle closes, Figure 4(d), the IOS includes the blue/green part of the light scatter appears (peak at 545 nm) and propagation begins, Figure 4(e). Because the red/near-infrared part of the IOS matches the field potential distribution, one can see that a circular current closes and initiates propagation. What was lacking was the semblance of the magnetic field associated with the circular current. To realize that a magnetic torus guided water and ions flow, we had first to make experiments with liquid deuterium [18] [19] and interpret these results in the light of the energy release at the wavefront. Second, we looked for experimental models that studied water release of energy in the form of electromagnetic flows, heat and mechanical flow of water. This model exists and is the subject of study of Elmar C. Fuchs and cols. [20] [Note 3].

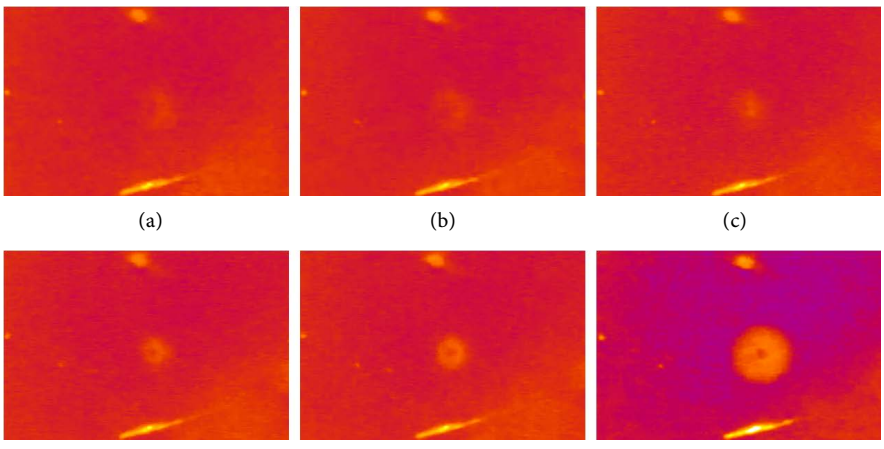

Figure 4. Transition from quiescence to excitation wave seen as changes in the IOS around the stimulated area (previous figure). (a) to (e) have a time interval of 200 msec, frame (f) is the same frame (f) is the same frame shown in the previous Figure 3. The frames adjusted for contrast with Image J software and the display of the 8 bits gray levels is in false colors. (a) to (c) show the standing pattern that precedes propagation. The IOS has only red/near-infrared wavelengths, at (d) a narrow circle closes and at this point, short wavelength components are present. The circle follows the potential distribution or the electrical field, hence a circular current induced; (e) propagation beguis. The illumination in the experiment made with a lamp with a flat emission spectrum between 400 - 600 nm.

First let us examine the liquid deuterium results. We applied liquid deuterium as the solvent in both isolated retinas and Belouzov-Zabotinsky reaction system. As was the case with similar comparative experiments [21] the response of both systems was very similar, both responded with collapse of excitability in a short time (2 hours). The pH of liquid water at 25 degrees Celsius is 7.0, the liquid deuterium pH is 7.4 or deuterium dissociation is five times smaller than that of liquid water dissociation. In our interpretation of the transition from quiescence to propagating wave, these results were not surprising as we first though, but the expected effect of the solvent physical properties changes. It should be noted that the classical HH membrane model does not either predict or explain the solvent deuterium effects, by contrast, Ichiji Tasaki model does [9].

Second, if we examine the flows in a water bridge, at the center, hydronium and hydroxyl ions run toward the cathode and anode electrodes, however twisting around the central current there is mass flow of liquid water and added particles configuring a torus [20]. In water bridges and CNS wavefronts, these charge and mass flows are coupled.

In summary, mechanical stimuli induce a dynamic standing pattern in which fluctuations in release of energy are amplified until a circular current form within the tissue, this current follows the electrical field. In parallel, a magnetic flow guides mass water and particles flow in the shape of a torus. This magnetic torus we propose as a key factor in spreading depression wave propagation.

We also reasoned that time series associated spatial propagation patterns in other parts of the CNS, had to be compatible with such patterns if our conjecture was correct, (see [22]). It was fortunate that in one study of propagation of spreading depression and after discharges, the sampling rate was 700 Hz, very unusual in ECoG recordings [10]. The geometry of the macroglial network in rat hippocampus is cylindrical and that is important. Here we assume that our interpretation about the role of the geometry of the macroglial network in the shape of spreading depression waves is correct [22]. Cylindrical geometry (think of windsocks in small airports) implies Von Karmann Street vortices, they in turn assumed to optimize the energy expenditure within the cylinder. If one measures this pattern in several points in the form of time series, then a split in frequencies should be present. Reexamining the data from the ECoG study [10] at the transition from after discharge to spreading depression, we found the pattern compatible with the expected frequency split of cylindrical geometry vortices. Our conjectures stand.

A further validation can look at vortices presence in excitable tissue and other electrochemical systems such as the B-Z system. Yes, vortices were found in heart tissue and B-Z [23] [24]. Besides these results, another set of experiments suggests vortex effects, non-stationary pathways in B-Z [25] and in isolated retinas [26]. In retinas, the sudden (step) change in potassium activity in the maintenance solutions from 6 to 1or 0 mEq/l, produces a hyper excitable pathway with a succession of spreading depression waves that terminate in tissue death in

about 30 minutes. These waves have altered IOSs. Last, but not least, the alteration of the isolated retinal solution by addition of the liquid glycerol adds viscosity and polarity to the retinal bath solution. The spread velocity, field potential and the IOS observed in the presence of glycerol differed from controls. The red/near infrared light scatter was present whereas the green component was depressed, the spread velocity was slower and voltage record changed kinetics with a prolonged plateau (see [4] [5] [12]). Once more, the electric equivalent model and molecular biology do not predict or explain these results. By contrast, interference with flows do.

3.2. Perceptual and Cognitive Correlates of Spreading Depression Waves

Lashley [6] used the scotomas (bright columns) march through his visual field to predict spreading depression waves as we said in the introduction section. Therefore, the knowledge that the frontwave distorts perception is as old as the wave discovery. Also it is long known that these wave have cognitive consequences in the form of learning and memory mechanisms blockage (for review see Bures, J.1974 [27] Sparks and Gallo, M. 2007 [28]); Bures and Buresova, 1963 [29]; Travis, R.P. and Sparks, D.L. 1963 [30]).

These cognitive impairments occur with structural reversible changes in the gels associated with membranes and energy expenditure in the form of heat and red/near infrared non-Plank dissipation, mass and charge flow. One question arises: is this the maximum rate of dissipation possible? Several sets of data about cortical and retinal waves appear to support that, indeed, this is the case. In the first 10 - 12 seconds of a wave one cannot distinguish between a reversible excitation wave and a non-reversible pathway to tissue death; see, for example [31]; later on, the pattern of spread and the irreversible character of an excitotoxic response makes them clearly distinct. The initial state of several pathways appears the same and thus, vortex effects will explain them all: the magnetic flow guides the mass (carried by liquid water) and charge flows.

Another question emerges: can resonances in the form of eddies of similar flows or Von Karmann street explain a perceptual phenomenon like the epiphanies?

Epiphanies with visualization of problems solutions exist in science. Famous are the ones related by August Kekule and the benzene ring and what Roger Penrose told about visualizing quasi-crystals before chemistry was aware of them [32]. What characterizes these perceptual states are the strong positive emotion (elation) and a strong memory trace let for recall, in contrast with the memory loss associated with the state at the frontwave of spreading depression waves. Here we speculate that an unusual resonant state could be present in the brain during the few seconds long insight period. The spatial shape of the resonances varying in different parts of the brain. The tubular spinal chord and brainstem candidates for Von Karman Street pattern.

Vortex effects appear to be the nature way of maximizing energy expenditure;

their expression present in weather phenomena like tropical storms and hurricanes. Storms can stay put or drift slowly, whereas hurricanes do travel, albeit with different velocities depending on many factors, among which the temperature gradient. The same mechanisms for energy expenditure are present in both phenomena. In the cylindrical rat hipocampus, we found the predicted frequencies split at the frontwaves of spreading depressions [10] [33], either this is a happy coincidence or vortex effects are indeed present in the brain.

4. Conclusions

Eighty years ago, Lashley and Leão inferred and discovered the spreading depression wave, a cortical excitation/inhibition that propagates at mm/min rate. What key factor rules spreading depression propagation remained an unsolved problem.

The visualization of the potential distribution at the quiescence/propagation transition in isolated retinas, led to a deduced circular current around the palisade formed by the glial network. We propose a torus of magnetic flow coupled to the circular current. This torus guides mass and charge transfer *i.e.* water and ions flows from excited to quiescent tissue recruiting new elements of membranes in the frontwave. At the back, the inverted flow is an important part of the absolute inhibition phase of the temporal evolution of tissue states: quiescent, excited, inhibited absolute, inhibited relative, quiescent.

A conjecture is only as good as its integrative power in explaining phenomena believed to be apart. Another aspect is its usefulness and this one can add new aspects to image interpretation in neurology and it will provide help in the interpretation of non-invasive magnetic brain stimulation effects.

Acknowledgments

Frank van den Bovenkamp for discussion in Research Gate, and Wolfgang Hanke for 30 years of friendship and partnership in the adventure of Science (VMFL), FAPESP (APJ).

Conflicts of Interest

The authors declare no conflicts of interest regarding the publication of this paper.

References

[1] Piralishvili, S.A. (2020) Vortex Effect: A History of Its Development in the USSR and Russia. *AIP Conference Proceedings*, **2211**, Article ID: 020004. https://doi.org/10.1063/5.0001006

[2] Fernandes de Lima, V.M. and Hanke, W. (2014) Relevance of Excitable Media Theory and Retinal Spreading Depression in Pre-Clinical Pharmacological Research. *Current Neuropharmacology*, **12**, 413-433. https://doi.org/10.2174/1570159X12666140630190800

[3] Fernandes de Lima, V.M. and Pereira Jr., A. (2016) The Plastic Glial-Synaptic Dy-

namics within the Neuropil: A Self-Organizing System Composed of Polyelectrolytes in Phase Transitions. *Neural Plasticity*, **2016**, Article ID: 7192427. https://doi.org/10.1155/2016/7192427

[4] Fernandes de Lima, V.M., Goldermann, M. and Hanke, W. (1999) The Retinal Spreading Depression. Shaker Verlag, Aachen, 209 p.

[5] Fernandes de Lima, V.M. and Hanke, W. (1997) Excitation Waves in Central Gray Matter: The Retinal Spreading Depression. *Progress in Retinal and Eye Research*, **16**, 657-690. https://doi.org/10.1016/S1350-9462(96)00038-9

[6] Lashley, K.S. (1941) Patterns of Cerebral Integration Indicated by the Scotomas of Migraine. *Archives of Neurology & Psychiatry*, **177**, 199-210.

[7] Tasaki, I. and Byrne, P.M. (1991) Heat Production Associated with Spreading Depression in the Amphibian Retina. *Biochemical and Biophysical Research Communications*, **174**, 293-297. https://doi.org/10.1016/0006-291X(91)90519-D

[8] Tasaki, I. and Byrne, P.M. (1992) Heat Production Associated with a Propagated Impulse in Bullfrog Myelinated Nerve Fibers. *The Japanese Journal of Physiology*, **42**, 805-813. https://doi.org/10.2170/jjphysiol.42.805

[9] Tasaki, I. (2008) On the Reversible Abrupt Structural Changes in Nerve Fibers Underlying Their Excitation and Conduction Processes. In: Pollack, G., Ed., *Phase Transitions in Cell Biology*, Springer Science Business Media, Berlin, 1-21. https://doi.org/10.1007/978-1-4020-8651-9_1

[10] Fernandes de Lima, V.M., Pijn, J.P., Felipe, C. and Lopes da Silva, F. (1990) The Role of Hippocampal Commissures in the Interhemispheric Transfer of Epileptiform after Discharges in the Rat: A Study Using Linear and Non-Linear Regression Analysis. *EEG and Clinical Neurophysiology*, **76**, 520-539. https://doi.org/10.1016/0013-4694(90)90003-3

[11] Dahlem, M. and Müller, S. (1997) Self-Induced Splitting of Spiral-Shaped Spreading Depression Waves in Chicken Retina. *Experimental Brain Research*, **115**, 319-324. https://doi.org/10.1007/PL00005700

[12] Fernandes de Lima, V.M. and Hanke, W. (2020) Reversibility of Excitation Waves in Brain and Heart and the Energy of Interfacial Water. Can Reversibility Be Explained by It? *Progress in Biophysics and Molecular Biology*.

[13] Nicholson, C. (1984) Comparative Neurophysiology of Spreading Depression in the Cerebellum. *Anais da Academia Brasileira de Ciências*, **56**, 481-494.

[14] Khmelinskii, I., Golubeva, T., Korneeva, E., Ynyushin, M., Zueva, L. and Makarov, V. (2017) Spectral Selectivity Model for Light Transmission by the Intermediate Filaments in Müller Cells. *Journal of Photochemistry and Photobiology B: Biology*, **173**, 282-290. https://doi.org/10.1016/j.jphotobiol.2017.06.001

[15] Bunkin, N., Gorelik, V.S., Koslov, V., Shkirin, A. and Suyazov, N.V. (2014) Colloidal Crystal Formation at the "Nafion-Water" Interface. *The Journal of Physical Chemistry B*, **118**, 3372-3377. https://doi.org/10.1021/jp4100729

[16] Franze, K., Groshe, J., Skatchkov, S.N., Shinkinger, S., Foja, C., Skild, D., Ukermann, O., Travis, K., Reichenbach, A. and Guck (2007) Müller Cells Are Living Optical Fibers in the Vertebrate Retina. *PNAS*, **194**, 8287-8292. https://doi.org/10.1073/pnas.0611180104

[17] Reichenbach, A. and Bringmann, A. (2010) Müller Cells in the Healthy and Diseaded Retina. Springer, New York, 91-97.

[18] Fernandes de Lima, V.M. and Hanke, W. (2011) Modulation of CNS Excitability by Water Movement. The D2O Effects on the Non-Linear Neuron-Glial Dynamics.

Journal of Bio-Physical Chemistry, **2**, 253-260.

[19] Klink, O., Hanke, W., Gerbershagen, E. and Fernandes de Lima, V.M. (2010) Influence of Heavy Water in the Belouzov-Zabotinsky Reaction. In: Petrin, A., Ed., *Wave Propagation in Materials for Modern Applications*, INTECH, Rijeka, 400-418.

[20] Fuchs, E.C., Agostinho, L.L.F., Eisenhut, M. and Woisetschlager, J. (2010) Mass and Charge Transfer within a Floating Water Bridge. *Proceedings of SPIE Laser Applications in Life Sciences*, Vol. 7376, 73761E. https://doi.org/10.1117/12.868994

[21] Hanke, W., Wiedemann, M. and Fernandes de Lima, V.M. (2002) Control of Excitability of Neuronal Tissue by Weak External Forces. *Faraday Discussions*, **120**, 237-248. https://doi.org/10.1039/b102706a

[22] Fernandes de Lima, V.M., Piqueira, J.R.C. and Hanke, W. (2014) The Tight Coupling and Non-Linear Relationship between the Macroscopic Electrical and Optical Concomitants of Electrochemical CNS Waves Reflect the Non-Linear Dynamics of Neural-Glial Propagation. *Open Journal of Biophysics*, **5**, Article ID: 51357. https://doi.org/10.4236/ojbiphy.2015.51001

[23] Cabo, C., Pertsov, A.M., Davidenko, J.M., Baxter, W.T., Gray, R.A. and Jalife, J. (1996) Vortex Shedding as a Precursor of Turbulent Electrical Activity in Cardiac Muscle. *Biophysical Journal*, **70**, 1105-1111. https://doi.org/10.1016/S0006-3495(96)79691-1

[24] Ginn, B.T. and Steinbock, O. (2005) Front Aggregation in Multiarmed Excitation Vortices. *Physical Review E*, **72**, Article ID: 046109. https://doi.org/10.1103/PhysRevE.72.046109

[25] Hanke, W. (1999) Inverse Dispersion Relation of B-Z Waves in Nonstationary Gels. *International Journal of Bifurcation and Chaos*, **9**, 2099-2104. https://doi.org/10.1142/S021812749900153X

[26] Dahlem, Y.A., Dahlem, M.A., Mair, T., Braun, K. and Müller, S.C. (2003) Extracellular Potassium Alters Frequency and Profile of Retinal Spreading Depression Waves. *Experimental Brain Research*, **152**, 221-228. https://doi.org/10.1007/s00221-003-1545-y

[27] Bures, J., Buresova, E. and Krivanek, J. (1974) The Mechanism and Applications of Leão's Spreading Depression of Electroencephalographic Activity. Academic Press, Cambridge.

[28] Gallo, M. (2007) Reversible Inactivation of Brain Circuits in Learning and Memory Research. In: Bermúdez-Rattoni, F., Ed., *Neural Plasticity and Memory: From Genes to Brain Imaging*, CRC Press/Taylor & Francis, Boca Raton, Chapter 8. http://www.ncbi.nlm.nih.gov/books/NBK3922 https://doi.org/10.1201/9781420008418.ch8

[29] Bures, J. and Buresova, O. (1963) Cortical Spreading Depression as a Memory Disturbing Factor. *Journal of Comparative and Physiological Psychology*, **56**, 268-272.

[30] Travis, R.P. and Sparks, D.L. (1963) The Influence of Unilateral and Bilateral Spreading Depression during a Learning upon Subsequent Relearning. *Journal of Comparative and Physiological Psychology*, **56**, 56-59. https://doi.org/10.1037/h0043538

[31] Fernandes de Lima, V.M. and Hanke, W. (2012) The Kinetics of Non-Synaptically Triggered Acute Excitotoxic Responses in the Central Nervous System Observed Using Intrinsic Optical Signals. *CNS and Neurological Disorders—Drug Targets*, **11**, 132-141. https://doi.org/10.2174/187152712800269704

[32] Penrose, R. (1991) The Emperor's New Mind. Penguim Books, New York, 435-437.

[33] Pijn, J.P., Vijn, P., Lopes da Silva, F. and Fernandes de Lima, V.M. (1989) Evolution of Interactions between Brain Structures during an Epileptic Seizure in a Kindled Rat. *EEG and Clinical Neurophysiology*, **73**, 172-178. https://doi.org/10.1016/0013-4694(89)90198-3

Notes

1) The IOS in the vertebrate retina is more than 90% of glial membrane activity; in the Gallus gender it is 98% or more. First, it is a vascular and there is no influence of blood vessels in the IOS. Besides the palisade architecture common to all vertebrate Müller cells, in the chick the cell body is divided in fine tubes (8 - 14) filled with closed apposed strands of Glial Fibrillary Acidic Protein (GFAP) in the inner retina (inner plexiform layer, ganglion cell layer and inner limiting membrane) each tube terminated with one end feet [5]. There are no organelles inside these tubes like mitochondria. At the external leaflet, the glial membrane has the EZ of the glycocalix, and at the internal leaflet, the EZ around the GFAP filaments; this EZ fills completely the filaments. Optically, the EZ behaviour is that of a quasi-liquid crystal with birefringence. [10] [12] and physiologically, each tube acts as light guide, the shape of the end feet acts as lens and the EZ a light channel. The current of an approaching wave will flow in the extracellular space above the end feet and around the cell bodies of the glia. The depolarization of the membrane relaxes the EZs at both sides and the cells loose transparency, increasing light scatter concomitant with loss of birefringence. Note that although tightly coupled, the two macroscopic variables are not causally related.

2) For the reader outside biology, a very good analogy of the rat hippocampus is a cashew nut. The head is the dorsal hippocampus and the smaller tail the ventral one. Each mammal has two hippocampi, in the rat the two dorsal heads are close and get apart so that the ventral end is well separated in the rat brain. If one cut the cashew in the frontal plane, what is seen is again two cylinders imbricated one called CA1/CA3 regions and the other Fascia Dentata. No wonder, therefore, that the cylindrical topology dominates the propagation pattern of seizures and spreading depressions. In the hippocampus as well as in the neocortex, the following rule of thumb applies: excitatory input for afar uses acetylcholine (Ach) as chemical mediator and the local circuit and association fibres use glutamate/aspartate and GABA as mediators. The faraway input of the hippocampi is from the septal area and the association input travels in the dorsal and ventral commissures.

3) Elmar C. Fuchs is the rediscoverer of the water bridge and studied in detail this dynamic structure both from experimental and theoretical treatment. The video recordings can be accessed from his homepage: ECFUCHS.com. Infrared cameras documented the torus flow of micro spheres around the bridge, exactly what one expected from the Vortex effect in one-dimensional systems. We quote "The water with Rhodamine B rapidly moved through the bridge, curling close underneath the water surface towards the cathode." … "When tracer particles were added for flow measurements using a laser Doppler anemometer and for visualization, the floating water bridge revealed a rotating outer layer," Woisetschlager et cols., Experiments in a floating water bridge (2010) experiments in fluids, 48: 121-131.